

Chemical doping effect in the LaRu_3Si_2 superconductor with a kagome lattice

Baoxuan Li, Sheng Li, and Hai-Hu Wen*

National Laboratory of Solid State Microstructures and Department of Physics, Collaborative Innovation Center of Advanced Microstructures, Nanjing University, Nanjing 210093, China

(Received 7 June 2016; revised manuscript received 25 July 2016; published 27 September 2016)

LaRu_3Si_2 is a superconductor with a kagome lattice and transition temperature of 7 K. By doping different rare-earth and transition-metal elements on the La and Ru sites, the evolution of superconductivity has been extensively investigated. It is found that, except for doping Fe to Ru sites, all other dopants with rare-earth (Y, Lu, and Ce) or transition metals (Ni, Cr, and Cu) seem to suppress superconducting transition temperature in LaRu_3Si_2 very slowly. The quick suppression of superconductivity by Fe doping can be described by the Abrikosov-Gorkov relation. By fitting and analyzing the magnetic susceptibility data under a high magnetic field with the Curie-Weiss law, we find that the effective magnetic moments for Ni and Cr doped samples are very small, indicating that these ions actually do not behave like strong magnetic scattering centers as Fe ions do in the present environment. Our experiments on systematically doped samples and related analysis indicate that the superconducting gap in LaRu_3Si_2 has no sign change.

DOI: [10.1103/PhysRevB.94.094523](https://doi.org/10.1103/PhysRevB.94.094523)**I. INTRODUCTION**

It is widely perceived that nonphonon mediated pairing should exist in many unconventional superconductors. After study for nearly half a century, physicists believe that the pairing glue may be related to the strong correlation effect or due to the enhanced spin fluctuations approaching some quantum critical points [1–5], although a unified and self-consistent picture for unconventional superconductivity is still lacking. In this regard, the RT_3Si_2 or RT_3B_2 (R=rare earth metal, T=transition metal) system offers a very interesting platform for us to study this important issue, since various chemical combinations are allowed in the present system, which gives us easy manipulation of the magnetic and superconductivity state. On the other hand, the kagome lattice formed by the transition metal naturally offers geometric frustrations, which may lead to strong magnetic fluctuations and even the potential quantum spin-liquid state [6], both of which are closely related to superconductivity [7,8]. In fact, superconductivity is very common in this 132 system, and almost ten superconductors have been found with this structure, for example, LaRh_3B_2 with $T_c \approx 2.8\text{K}$ [9], CeOs_3B_2 with $T_c \approx 3.5\text{K}$ [10], ThIr_3B_2 with $T_c \approx 2.1\text{K}$ [11], CeRu_3Si_2 with $T_c \approx 1\text{K}$ [12], and so on. Among them, LaRu_3Si_2 has the highest transition temperature of about 7 K [13].

The previous specific-heat measurement for LaRu_3Si_2 has revealed some correlation effect in this system, and the field dependence of the induced quasiparticle density of states (DOS) shows a nonlinear feature, indicating the significant contribution given by the delocalized quasiparticles [14] near the gap minimum or nodes. All these results suggest that LaRu_3Si_2 has probably some features of unconventional superconductivity. Previous study shows that doping Fe on Ru sites totally suppresses superconductivity with merely 3% doping level, and introduces spin-polarized electrons leading to strong localized magnetic moments. However, doping Co suppresses superconductivity very slowly without

introducing clear magnetic moments [15]. In this paper, we try to substitute with other rare-earth and transition-metal elements on the La or Ru sites, expecting to get a deeper insight into superconductivity in the LaRu_3Si_2 system.

II. EXPERIMENTAL DETAILS

The LaRu_3Si_2 samples were synthesized by arc-melting method. High-purity La chunk (purity 99.9%, Cuibolin), Ru powder (purity 99.9%, Alfa Aesar), and Si powder (purity 99.9%, Alfa Aesar) were weighed, mixed well, and pressed into a pellet in an argon filled glove box. In order to avoid the formation of the LaRu_2Si_2 phase, we intentionally used some exceeding amount of Ru metal by about 15% in the starting materials, so the nominal compositions should be $\text{LaRu}_{3.45}\text{Si}_2$. To achieve the homogeneity, three rounds of welding with the alternative upper and bottom side of the pellet were taken in a vacuum electric arc furnace. The doped samples were fabricated by the same synthesized procedure, using $\text{La}(\text{Ru}_{1-x}\text{T}_x)_{3.45}\text{Si}_2$ and $\text{La}_{1-x}\text{R}_x\text{Ru}_{3.45}\text{Si}_2$ as the nominal compositions.

X-ray-diffraction (XRD) measurements were performed on a Bruker D8 Advanced diffractometer with the $\text{Cu} - \text{K}_\alpha$ radiation. Energy dispersive x-ray spectrum measurements were performed at an accelerating voltage of 20 kV and working distance of 10 mm by a scanning electron microscope (Hitachi Co., Ltd.). The dc magnetization measurements were carried out by using a SQUID-VSM-7T (Quantum Design) with a resolution of about 5×10^{-8} emu. Measurements of resistivity were performed on a physical property measurement system (PPMS-16T, Quantum Design) with the dc resistivity and ac transport options. For the resistive measurements, gold wires with a diameter of $50 \mu\text{m}$ were glued to the doped LaRu_3Si_2 sample in a standard four-probe method by using silver epoxy.

III. RESULTS AND DISCUSSION

Figure 1(a) shows the powder XRD patterns of the LaRu_3Si_2 sample at room temperature, along with the result

*hhwen@nju.edu.cn

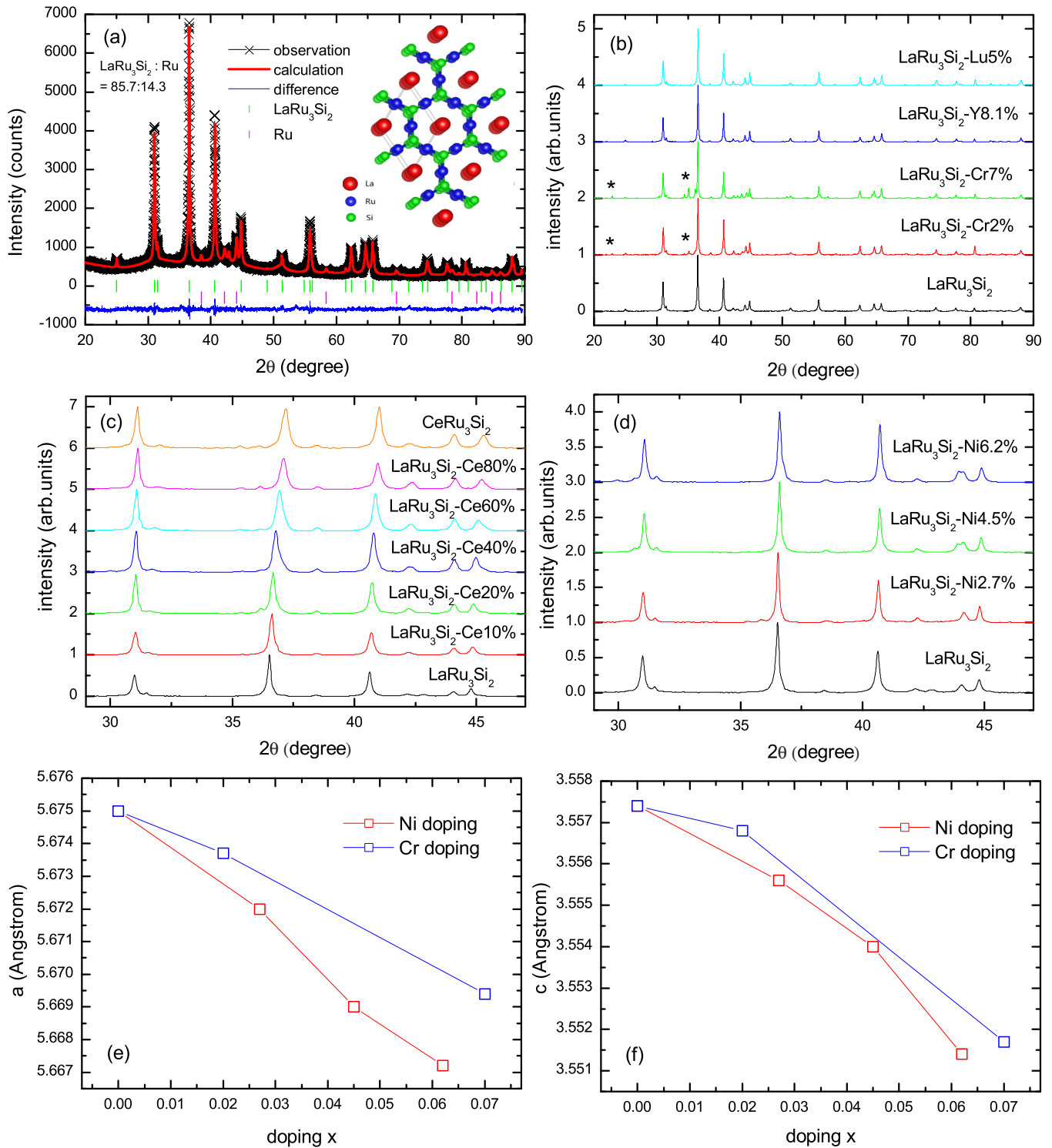


FIG. 1. (a) Powder x-ray-diffraction patterns and the Rietveld refinement profile of the LaRu_3Si_2 sample at room temperature. All main diffraction peaks can be indexed well by the $P6/mmm$ space group (hexagonal structure) with $a = 5.675 \text{ \AA}$ and $c = 3.557 \text{ \AA}$ with the excess Ru as the impurity phase. The ratio between LaRu_3Si_2 and the Ru impurity is found to be 85.7:14.3. (b) X-ray-diffraction patterns for Ce doped LaRu_3Si_2 samples. (c) X-ray-diffraction patterns for Cr doped and Ln doped LaRu_3Si_2 samples. (d) X-ray-diffraction patterns for Ni doped LaRu_3Si_2 samples. (e) The evolution of the a -axis lattice constants for Ni- and Cr doped samples vs the doping concentration. (f) The evolution of the c -axis lattice constants for Ni- and Cr-doped samples vs the doping concentration.

of the Rietveld structural refinement using the TOPAS program. In general, it is clear that the main diffraction peaks can be indexed well by a hexagonal cell structure with the $P6/mmm$ space group. In addition to the LaRu_3Si_2 phase, some weak

peaks from impurity can also be seen; they come from the 15% excess of Ru which is added in the starting material. A detailed fitting to the structural data shows that the ratio between LaRu_3Si_2 and Ru is around 85.7:14.3 for the present

TABLE I. Energy dispersive x-ray microanalysis results for some doped LaRu_3Si_2 samples. Cr-A and Cr-B stand for the two Cr doped samples with different doping levels, and the same for Ni doping.

Cr-A		Cr-B		Ni-A		Ni-B		Lu		Y	
Nominal	5%	Nominal	10%	Nominal	5%	Nominal	8%	Nominal	5%	Nominal	10%
S1	2.0%	S1	6.4%	S1	4.1%	S1	7.2%	S1	5.3%	S1	8.4%
S2	2.4%	S2	7.6%	S2	4.4%	S2	5.9%	S2	4.8%	S2	8.2%
S3	1.7%	S3	7.1%	S3	5.0%	S3	5.6%	S3	5.4%	S3	7.7%

sample, which is very close to the original proportion. The refined lattice parameters are extracted to be $a = 5.675\text{\AA}$ and $c = 3.557\text{\AA}$. In Fig. 1(a), we also show the lattice structure of LaRu_3Si_2 ; apparently the Ru atoms form a honeycomblike kagome lattice, which exhibits very strong geometric frustration.

We also present the powder XRD patterns for all the doped LaRu_3Si_2 samples at room temperature in Figs. 1(b)–1(d). One can see that the positions of the main peaks evolve systematically with increasing the doping level. We have enlarged some peaks for Ce and Ni substitution series in Fig. 1(c) and 1(d) to highlight this evolution. Apart from the Cr doped samples, which have some peaks arising from La and Ru_4Si_3 impurities as marked in Fig. 1(b), other doped samples seem to be very pure comparing with the LaRu_3Si_2 parent phase. The fitting lattice constants of a and c axes in Cr and Ni doped samples are shown in Figs. 1(e) and 1(f), respectively. We find that the a and c lattice parameters decrease monotonously upon doping Cr or Ni, which is understandable since the radius of Cr or Ni ion is smaller than that of the Ru ion. The systematic evolvments of the lattice constants indicate that the Cr or Ni ion has already been doped into the kagome lattice.

In order to determine the real doping levels of the doped samples, we also did scanning electron microscope measurements; some of the energy dispersive x-ray microanalysis results for the doped LaRu_3Si_2 samples are shown in Table I. To ensure homogeneity, we have measured each sample at three different positions marked as 1, 2, and 3 in Table I, and the actual doping level for one sample is obtained by averaging these three values. We can see that the distribution of dopants in one sample is relatively uniform, although the actual doping level is lower than the nominal one.

Figure 2 shows the resistivity and dc susceptibility zero-field-cooled and field-cooled measurements under 50 Oe for samples with doping from LaRu_3Si_2 to CeRu_3Si_2 ; the latter is also a superconductor with $T_c \approx 1\text{ K}$ [12]. Here we do not take the demagnetization factors into consideration, so some of the magnetization expressed by $4\pi\chi$ are larger than 1 at low temperatures. The same is applied to the magnetic susceptibility data shown in subsequent figures. We notice that the 40 and 60% Ce doped samples have the largest residual resistivity, which is caused by the strongest disorder here. The suppression of superconducting transition temperature T_c is shown in Fig. 6(a), with the transition temperature for CeRu_3Si_2 obtained from the previous report [12]. We can see that the transition temperature decreases monotonously with doping Ce ions. Figure 3 shows the resistivity and dc susceptibility measurements under 50 Oe for $\text{La}(\text{Ru}_{1-x}\text{Ni}_x)_3\text{Si}_2$ samples. We can see that the superconducting transition

becomes broader upon doping in the magnetic susceptibility curves. The primary reason may be that the impurity scattering would spontaneously induce some density of states within the superconducting gap [16]. Apparently the transition temperature decreases monotonously with Ni doping, which indicates that the Ni impurities acting as scattering centers would be harmful to the Cooper pairs. However, at the highest doping level of about 6.2%, the transition temperature only decreases from 6.9 K of the parent phase to about 4.8 K. The suppression to superconductivity seems to be much weaker than that in the Fe doped samples. Figure 4 shows the resistivity and dc susceptibility under 50 Oe for $\text{La}(\text{Ru}_{1-x}\text{Cr}_x)_3\text{Si}_2$ samples.

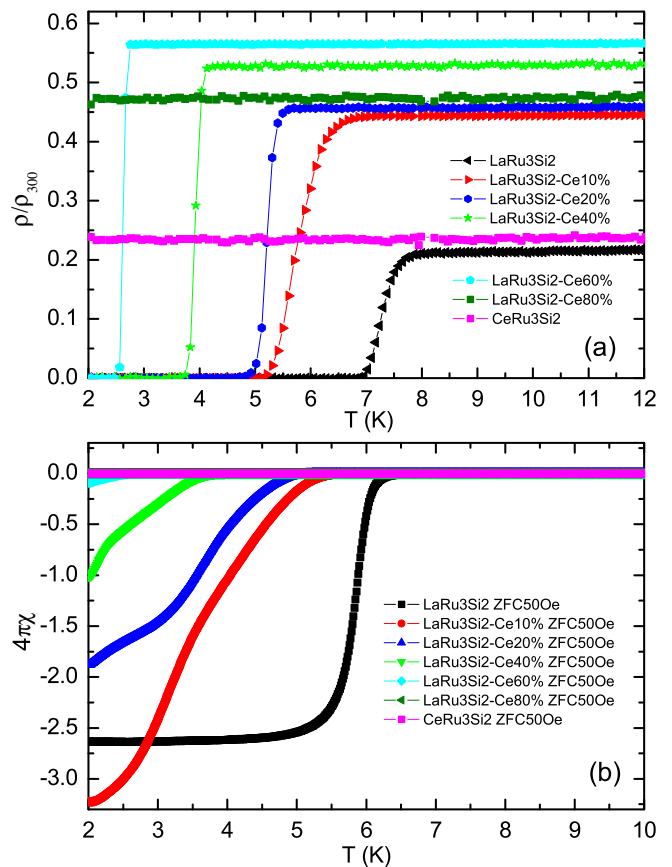


FIG. 2. (a) Temperature dependence of electrical resistivity for samples doping from LaRu_3Si_2 to CeRu_3Si_2 around the transition temperature. (b) Temperature dependence of dc magnetic susceptibility for samples doping from LaRu_3Si_2 to CeRu_3Si_2 as measured under a magnetic field of 50 Oe. Both the magnetic susceptibilities measured in zero-field-cooled (ZFC) and field-cooled (FC) modes are shown. The value of $-4\pi\chi$ measured with the ZFC mode is larger than 1 because of the demagnetization factor.

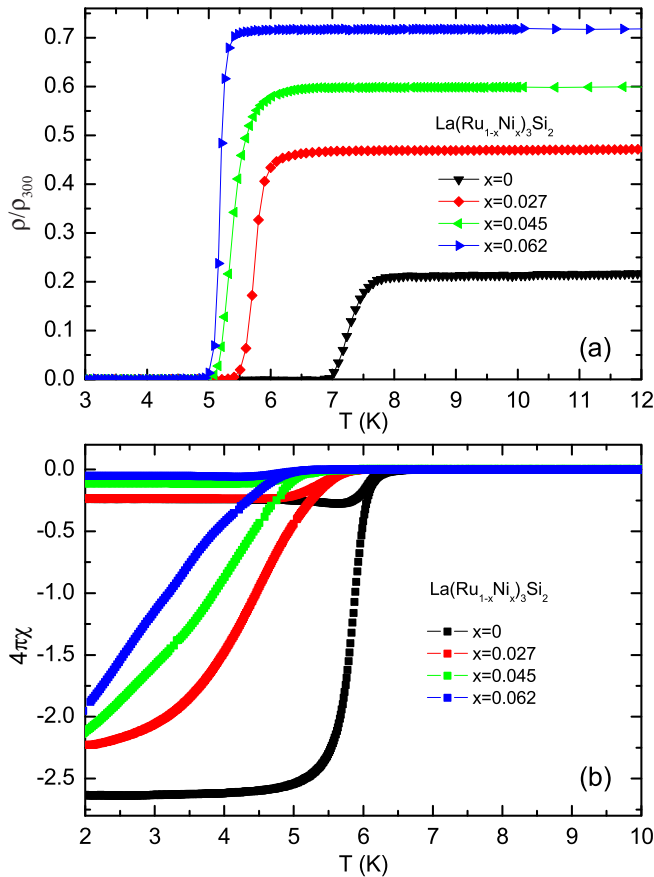


FIG. 3. (a) Temperature dependence of electrical resistivity for Ni doped LaRu_3Si_2 samples around the transition temperature. (b) Temperature dependence of dc magnetic susceptibility for Ni doped LaRu_3Si_2 samples as measured under 50 Oe. Both the magnetic susceptibilities measured in zero-field-cooled (ZFC) and field-cooled (FC) modes are shown.

We find that the suppression to superconductivity in doping Cr dopants is similar to that in Ni doped samples. With increasing the doping level to 7.0%, the transition temperature drops to about 4.9 K. Figure 5 shows the resistivity and dc susceptibility under 50 Oe for $\text{La}_{1-x}\text{R}_x\text{Ru}_3\text{Si}_2$ ($\text{R} = \text{Lu}, \text{Y}$) samples. It seems that the suppression of superconductivity with rare-earth substitution in the 132 system is very slow. The transition temperature is only suppressed to 6.2 and 6.1 K with 5.2% Lu and 8.1% Y doping level, respectively. The T_c declining rate is in fact similar to that of the Ce doped samples.

In Fig. 6, we present the obtained transition temperatures for all the doped samples. The transition temperatures are determined by the point of zero resistance, which roughly corresponds to the onset transition point of the diamagnetic signal. The transition temperatures for Fe doped samples are obtained from the previous measurements [15]. As we can see, although the Ni and Cr doped on Ru sites can suppress superconductivity, the suppression rate is actually close to that of the Co doped samples, and much weaker than that in the Fe doped samples. In the inset of Fig. 6(a), we also show the correlation between the residual resistivity at low temperatures versus doping level for different substitution series. We find

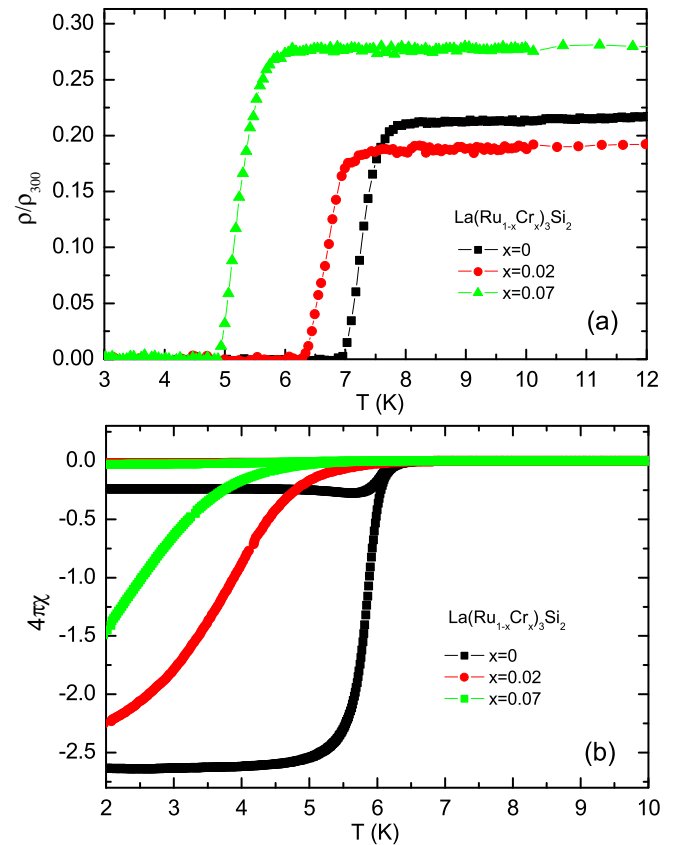


FIG. 4. (a) Temperature dependence of electrical resistivity for Cr doped LaRu_3Si_2 samples around the transition temperature. (b) Temperature dependence of dc magnetic susceptibility for Cr doped LaRu_3Si_2 samples as measured under 50 Oe. Both the magnetic susceptibilities measured in zero-field-cooled (ZFC) and field-cooled (FC) modes are shown.

that the residual resistivity increases with doping because of the enhancement of disorder scattering. In particular, the residual resistivity for Ni doped samples increases much faster than that for the Fe substitution series, although Ni dopants do not strongly destroy superconductivity as Fe dopants do. Referring to the result from Li *et al.* [15], we notice that the residual resistivity increases monotonously with doping on Ru sites by elements from left to right (Cr, Fe, Co, Ni) in the periodic table. This phenomenon may be explained in a way that the charge carriers are holelike, so the carrier density would decrease with doping more d electrons into the system. Moreover, we can see a minor decrease of the residual resistivity for the 2% Cr doped sample in the inset; this could be the result of the competition between the enhancement of disorder scattering and increase of the carrier density.

According to the Abrikosov-Gorkov (AG) theory [17] for the pair-breaking effect, the transition temperature is suppressed upon scattering rate or roughly with the density of doping impurities as the following [18,19]:

$$\ln\left(\frac{T_{c0}}{T_c}\right) = \psi\left(\frac{1}{2} + \frac{\alpha T_{c0}}{2\pi T_c}\right) - \psi\left(\frac{1}{2}\right), \quad (1)$$

where ψ is the digamma function, $\alpha = 1/2\tau T_{c0}$ is the pair-breaking parameter which is proportional to the doping level x ,

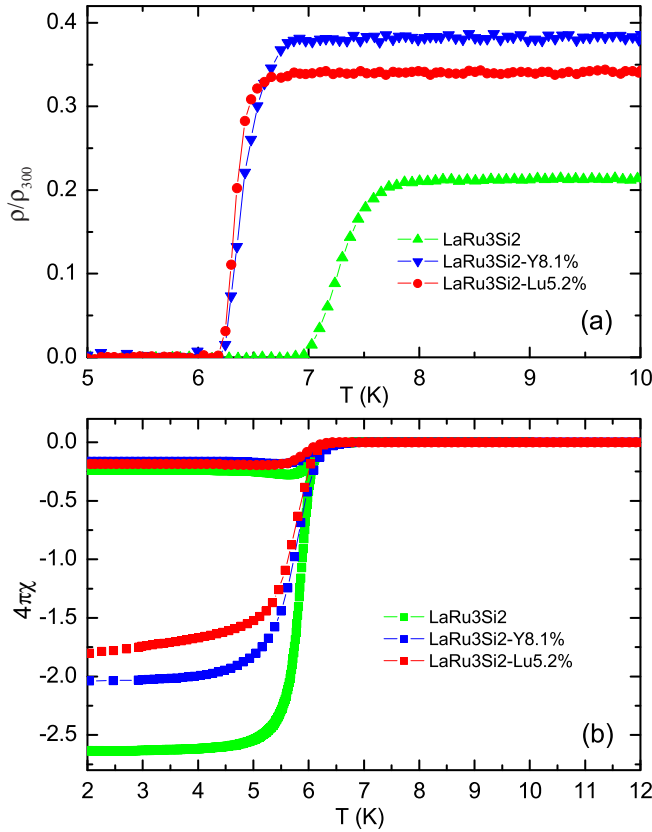


FIG. 5. (a) Temperature dependence of electrical resistivity for Ln doped LaRu_3Si_2 samples around the transition temperature. (b) Temperature dependence of dc magnetic susceptibility for Ln doped LaRu_3Si_2 samples as measured under 50 Oe. Both the magnetic susceptibilities measured in zero-field-cooled (ZFC) and field-cooled (FC) modes are shown.

and T_{c0} is the transition temperature of the parent phase. For the Fe doped samples, the fitting curve according to the AG theory is shown as the dashed line in Fig. 6(b). As one can see, the transition temperatures versus doping levels are in accordance with the AG theory. However, for all other dopants, the T_c - x curves are obviously deviated from the Abrikosov-Gorkov theory. Generally speaking, if the LaRu_3Si_2 superconductor has nodes on the SC gap, like the d -wave cuprates, both the magnetic and the nonmagnetic impurities should lead to the pair breaking, and the T_c versus the scattering rate should follow the AG behavior. So our results to some extent imply that the LaRu_3Si_2 superconductor may have a full gap without any sign change. In many systems, Cr and Ni elements hold strong magnetic moments, as Fe ions do. Therefore it is curious to know whether all other dopants give the same or different effect as the Fe ions.

In order to check the magnetic moments of the other dopants, we did the susceptibility measurement under 3 T for Ni and Cr doped samples, and fit the data from T_c to 30 K by using the Curie-Weiss law

$$\chi = \chi_0 + \frac{C}{T + T_0}, \quad (2)$$

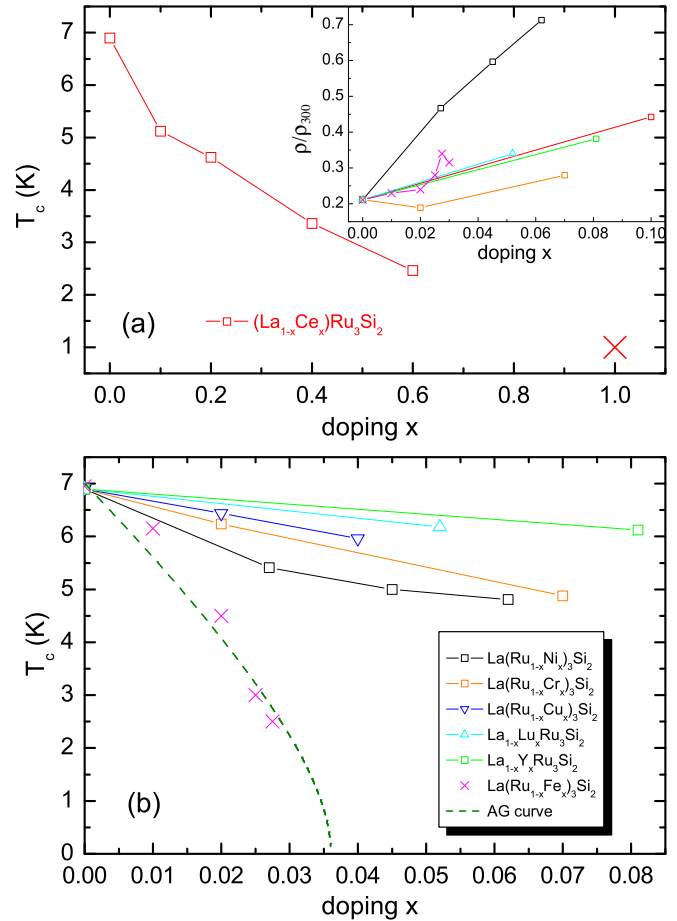


FIG. 6. (a) The transition temperatures for $(\text{La}_{1-x}\text{Ce}_x)\text{Ru}_3\text{Si}_2$ at different doping levels of Ce. The red cross at the doping level of $x = 1$ represents the data for CeRu_3Si_2 . The inset shows the normal state resistivity just above T_c normalized by the resistivity at 300 K for each sample. (b) The transition temperatures for rare-earth and transition-metal doped LaRu_3Si_2 samples.

where $C = \mu_0\mu_{\text{eff}}^2/3k_B$, χ_0 , and T_0 are fitting parameters. The parameter χ_0 comes from the Pauli paramagnetic term of the conducting electrons, while the temperature-dependent term comes from the localized magnetic moments, which will be significantly enhanced upon doping. In the fitting process, we leave these three parameters totally free. Some susceptibility data under 3 T along with the fitting curves are shown in Fig. 7. The relatively small fitting range (from T_c to 30 K) may bring about some uncertainties in terms of three fitting parameters. In principle, the small fitting range would reduce the influence of the change of χ_0 , induced by the variation of DOS at the Fermi level over a wider temperature range. From the fitting parameter C for the parent phase LaRu_3Si_2 , we can obtain the effective magnetic moment for Ru atoms, which arrives at $0.105\mu_B/\text{Ru}$. By subtracting the background magnetic moment of Ru atoms, we can obtain the effective magnetic moment for the samples doped with Ni or Cr atoms. The fitting parameters C and T_0 and the calculated effective magnetic moments μ_{eff} are listed in Table II. Simultaneously, we also calculated the effective magnetic moment of the 10% Ce doped sample, which arrives at $0.118\mu_B/(\text{La}_{0.9}\text{Ce}_{0.1}\text{Ru}_3\text{Si}_2)$.

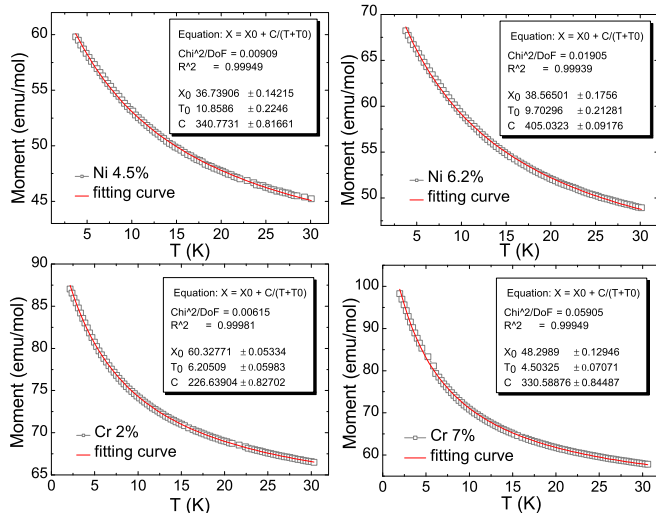


FIG. 7. The susceptibility data under 3 T from T_c to 30 K along with the fitting curves for some Ni and Cr doped samples; the obtained fitting parameters C , T_0 , and χ_0 are also shown.

This value is very close to $0.105\mu_B$ for the parent phase. This indicates that Ce doping in this 132 system should be nonmagnetic substitution, and the most observed magnetic moment for the 10% Ce doped sample may arise from the Ru sites.

In Fig. 8, we present the calculated effective magnetic moments of Cr, Ni, Co, and Fe dopants. The data for Ni and Cr come from the present experiment, while the results for Fe and Co are derived from the previous work [15]. One can see that the effective magnetic moments of Cr and Ni dopants are not very large, and the values are very close to that of the Co dopants. The largest effective magnetic moments of Ni and Cr dopants are $\mu_{\text{eff}}/\text{Ni} = 0.711\mu_B$ and $\mu_{\text{eff}}/\text{Cr} = 0.683\mu_B$, with doping levels of 2.7 and 2.0%, respectively. These values are apparently much smaller than that of the Fe dopant, which reaches $\mu_{\text{eff}}/\text{Fe} = 1.51\mu_B$ with a doping level of 2.75%. The fitting and calculated results can consistently explain the suppression effect to superconductivity in this system. It seems that the Cr and Ni dopants only provide very weak magnetic moments. Our self-consistent results of the suppression to superconductivity by the dopants, and the different magnetic moments derived from the data, suggest that the superconducting gap has no sign change. This rules out the possibility of d -wave or s_{\pm} gap in the system. In many

TABLE II. The fitting parameters C and T_0 and the calculated effective magnetic moments μ_{eff} for different doped LaRu_3Si_2 samples.

Dopant	$C(\text{K emu/mol})$	$T_0(\text{K})$	$\mu_{\text{eff}}(\mu_B)$
Ru	124.20	8.13	0.105
2.7%Ni	274.67	7.04	0.711
4.5%Ni	340.77	10.86	0.662
6.2%Ni	405.03	9.70	0.643
2.0%Cr	226.64	6.21	0.683
7.0%Cr	330.59	4.50	0.490

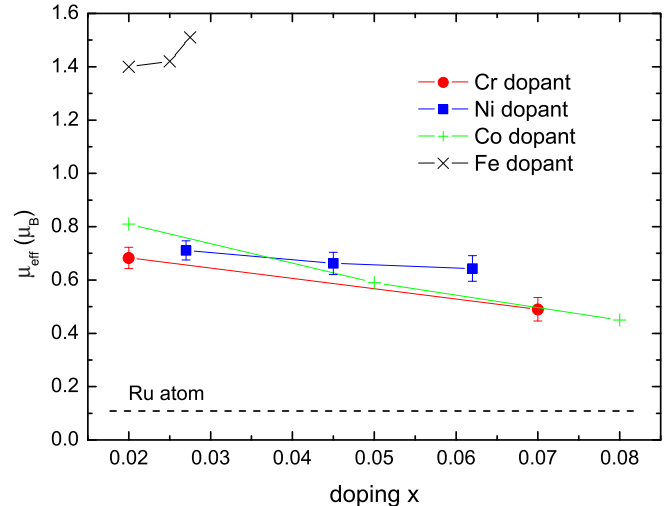


FIG. 8. The calculated localized effective magnetic moments of Ni and Cr dopants; the results for Fe and Co dopants are also shown for comparison. The dashed line represents the effective magnetic moments of one Ru atom.

systems, the Ni and Cr ions would also carry rather strong magnetic moments as Fe ions do. However, in the LaRu_3Si_2 system, apparently their magnetic moments are delocalized. It still remains unclear why the Fe impurities behave in such a unique way in this 132 system with a kagome lattice.

IV. CONCLUSION

In conclusion, by doping different rare-earth and transition metals on the La and Ru sites in LaRu_3Si_2 , we obtain the transition temperatures in wide doping ranges and find that all the dopants except for Fe suppress superconductivity slowly. We have also derived a phase diagram for the systematically Ce doped samples $\text{La}_{1-x}\text{Ce}_x\text{Ru}_3\text{Si}_2$. By fitting and analyzing the magnetic susceptibility data under a high magnetic field with the Curie-Weiss law, we find that the effective magnetic moments for Ni and Cr dopants are quite small. This indicates that Ni and Cr ions actually do not exhibit a very strong localized magnetic scattering effect as Fe ions do, and may only provide some itinerant electrons. The self-consistent results of the magnetic moments by different dopants and the distinct suppression rate to superconductivity suggest that the superconducting gap in LaRu_3Si_2 should have no sign change. It is interesting that the Fe impurities behave very uniquely and distinctly compared with other dopants in the present system.

ACKNOWLEDGMENTS

We thank X. Y. Zhu for his assistance in revising the manuscript. This work is supported by the National Natural Science Foundation of China with Projects No. A0402/11534005 and No. A0402/11190023, the Ministry of Science and Technology of China (Grants No. 2016YFA0300404, No. 2011CBA00100, and No. 2012CB821403), and Project Funded by the Priority Academic Program Development of Jiangsu Higher Education Institutions.

- [1] M. M. Qazilbash, J. J. Hamlin, R. E. Baumbach, L. J. Zhang, D. J. Singh, M. B. Maple, and D. N. Basov, *Nat. Phys.* **5**, 647 (2009).
- [2] M. R. Norman, *J. Supercond. Nov. Magn.* **25**, 2131 (2012).
- [3] B. Keimer, S. A. Kivelson, M. R. Norman, S. Uchida, and J. Zaanen, *Nature* **518**, 179 (2015).
- [4] C. M. Varma, Z. Nussinov, and W. van Saarloos, *Phys. Rep.* **361**, 267 (2002).
- [5] Z. P. Yin, K. Haule, and G. Kotliar, *Nat. Mater.* **10**, 932 (2011).
- [6] S. Yan, A. H. David, and R. W. Steven, *Science* **332**, 1173 (2011).
- [7] P. W. Anderson, *Science* **235**, 1196 (1987).
- [8] P. W. Anderson, P. A. Lee, M. Randeria, T. M. Rice, N. Trivedi, and F. C. Zhang, *J. Phys.: Condens. Matter* **16**, R755 (2004).
- [9] S. K. Malik, A. M. Umarji, G. K. Shenoy, A. T. Aldred, and D. G. Niarchos, *Phys. Rev. B* **32**, 4742 (1985).
- [10] K. S. Athreya, L. S. Hausermann-Berg, R. N. Shelton, S. K. Malik, A. M. Umarji, and G. K. Shenoy, *Phys. Lett. A* **113**, 330 (1985).
- [11] H. C. Ku, G. P. Meisner, F. Acker, and D. J. Johnston, *Solid State Commun.* **35**, 91 (1980).
- [12] U. Rauchschwalbe, W. Lieke, F. Steglich, C. Godart, L. C. Gupta, and R. D. Parks, *Phys. Rev. B* **30**, 444(R) (1984).
- [13] J. M. Vandenberg and H. Barz, *Mater. Res. Bull.* **15**, 1493 (1980).
- [14] S. Li, B. Zeng, X. G. Wan, J. Tao, F. Han, H. Yang, Z. H. Wang, and H.-H. Wen, *Phys. Rev. B* **84**, 214527 (2011).
- [15] S. Li, J. Tao, X. G. Wan, X. X. Ding, H. Yang, and H.-H. Wen, *Phys. Rev. B* **86**, 024513 (2012).
- [16] T. Michael, *Introduction to Superconductivity* (McGraw-Hill, Inc. New York, 1996).
- [17] A. A. Abrikosov and L. P. Gorkov, *Zh. Eksp. Teor. Fiz.* **39**, 1781 (1960).
- [18] H. Kim, G. Preosti, and P. Muzikar, *Phys. Rev. B* **49**, 3544 (1994).
- [19] R. J. Radtke, K. Levin, H.-B. Schuttler, and M. R. Norman, *Phys. Rev. B* **48**, 653 (1993).